

An analysis of the Ap binary HD 81009^{*}

G.A. Wade^{1,2}, Y. Debernardi³, G. Mathys⁴, D.A. Bohlender⁵, G.M. Hill⁶, and J.D. Landstreet⁷

¹ Astronomy Department, University of Toronto at Mississauga, Mississauga, Ontario, L5L 1C6, Canada

² Département de Physique, Université de Montréal, CP 6128, succ. Centre-Ville, Montréal, Québec, H3C 3J7, Canada

³ Institut d'Astronomie, Université de Lausanne, 1290 Chavannes-des-bois, Switzerland

⁴ European Southern Observatory, Casilla 19001, Santiago 19, Chile

⁵ Herzberg Institute of Astrophysics, Dominion Astrophysical Observatory, 501 West Saanich Road, Victoria, B.C., V8X 4M6, Canada

⁶ Hobby-Eberly Telescope, McDonald Observatory, P.O. Box 1337, Fort Davis, TX 79734, USA

⁷ Physics and Astronomy Department, University of Western Ontario, London, Ontario, N6A 3K7, Canada

Received 25 April 2000 / Accepted 24 July 2000

Abstract. We present a detailed investigation of the orbit, component characteristics and magnetic field of the single spectrum (SB1), visual Ap binary HD 81009.

By simultaneously modeling new and archival radial velocity measurements and new and archival speckle interferometric measurements (obtained with the CHARA array) we obtain a unique model of the orbital geometry and constraints on the component masses of HD 81009. Additional constraints provided by the Hipparcos parallax and component magnitude difference and the optical spectral energy distribution allow us to determine a self-consistent solution for the basic physical properties of the components. HD 81009 is a highly eccentric ($e = 0.718$), long-period ($P_{\text{orb}} = 29.3$ y) binary composed of two main sequence A-type stars. While its presence is required in order to explain the astrometric and photometric observations, the cooler secondary component is never detected spectroscopically, and is therefore inferred to rotate somewhat more rapidly than the hotter component.

The hotter primary component is identified as the slowly-rotating ($P_{\text{rot}} = 33^{\text{d}}984$) magnetic Ap star. We have modeled the magnetic field geometry of this star using new and archival longitudinal magnetic field and mean magnetic field modulus observations. The rotational variations of the magnetic quantities are consistent with a decentered dipole surface magnetic field geometry with small magnetic obliquity ($\beta < 20^\circ$). This is consistent with the observation of Landstreet & Mathys (2000), who report that nearly all magnetic Ap stars with periods longer than around 25 days exhibit $\beta < 20^\circ$, implying that their magnetic fields are approximately aligned with their rotational axes.

Key words: polarization – stars: binaries: general – stars: chemically peculiar – stars: individual: HD 81009 – stars: magnetic fields

1. Introduction

The magnetic, chemically peculiar A and B type stars (or Ap stars) comprise about 5–10% of all main sequence stars with spectral types F0-B2. The frequency of detected binary and multiple systems among these objects is only about one-half that observed for chemically “normal” F-B stars (Abt & Snowden 1973). This may result from observational selection, as the orbital period distribution of Ap binaries appears to be strongly skewed to long and very long periods (e.g. Mathys et al. 1997). The deficiency of short periods is particularly evident in the scarcity of double-lined spectroscopic binaries among the Ap stars; only 4 are known to exist (HD 98088 Abt et al. 1968, HD 55719 Bonsack 1976, HD 59435 North 1994; Wade et al. 1996 and HD 37017 Bolton et al. 1998). The clear connection between binarity and Ap stars has the potential to provide us with crucial insight into the physical processes responsible for magnetism and chemical peculiarity on the upper main sequence.

Toward this end we have undertaken a study of HD 81009 (=HR 3724=KU Hya), a visual binary (ADS 7334; Aitken 1929) with components of similar magnitude and separated by less than 0.2 arcsec. The combined spectral type is provided by Cowley et al. (1969) as A5p SrCrEu, although somewhat earlier spectra types have been published (e.g. A3p according to Abt 1981). It is a single-lined spectroscopic system; detection of the lines of the secondary has never been reported. The orbit and component characteristics have been studied for over 60 years with inferred orbital periods ranging over a factor of nearly 3, from around 22 years to 59 years. Mathys (1990) conducted an analysis of the available solutions and found that of Starikova (1981) to be most consistent with recent radial velocity observations. This solution indicates that the orbital period of HD 81009 is 53.4 y, and that the individual stellar components have very similar masses.

One component of HD 81009 is a magnetic Ap star with very narrow lines, some of which are split and resolved into their individual Zeeman components (Mathys et al. 1997). Mathys et al. (1997) reported 39 measurements of the mean magnetic field modulus of HD 81009, inferred from its magnetically split

Send offprint requests to: G.A. Wade (wade@astro.umontreal.ca)

^{*} Based on observations obtained at the European Southern Observatory (La Silla, Chile), the Haute Provence and Pic du Midi Observatories (France), and the Las Campanas Observatory (Chile)

Table 1. Journal of UWO longitudinal magnetic field observations of HD 81009. Phases are calculated from the ephemeris cited in Sect. 5.1 and σ_B is the 1 standard deviation uncertainty. Each measurement has been corrected for flux dilution due to the secondary in the manner described in Sect. 2.1.1

| JD-240 0000 | UWO | |
|-------------|-------|---------------------------|
| | Phase | $B_\ell \pm \sigma_B$ (G) |
| 47943.699 | 0.821 | 993 \pm 535 |
| 47951.688 | 0.056 | 1032 \pm 600 |
| 47971.645 | 0.643 | 3132 \pm 597 |
| 47976.672 | 0.791 | 2790 \pm 628 |
| 47978.664 | 0.850 | 1546 \pm 600 |
| 48025.484 | 0.227 | 1617 \pm 480 |
| 48028.469 | 0.315 | 2106 \pm 480 |
| 48327.711 | 0.121 | 1468 \pm 445 |
| 48328.648 | 0.148 | 1813 \pm 379 |
| 48331.707 | 0.238 | 2163 \pm 461 |
| 48718.629 | 0.624 | 2523 \pm 565 |
| 48725.637 | 0.830 | 2437 \pm 607 |
| 49020.797 | 0.515 | 3012 \pm 940 |
| 49023.770 | 0.603 | 2887 \pm 840 |
| 49053.680 | 0.483 | 2719 \pm 564 |
| 49745.766 | 0.848 | 781 \pm 470 |
| 50170.684 | 0.351 | 2566 \pm 600 |
| 50184.609 | 0.761 | 2650 \pm 489 |

Fe II 6149.2 Zeeman doublet, which sample the entire rotational cycle of the star.

In this paper we employ new and previously published astrometric, spectroscopic and polarimetric observations of HD 81009 to determine the system orbital geometry and the individual component characteristics, including the geometry of the magnetic field of the Ap star. In Sect. 2 we describe the new longitudinal magnetic field, radial velocity and spectroscopic measurements. We also briefly describe the previously published field modulus, astrometric, spectroscopic and photometric observations employed in our analysis. In Sect. 3 we determine the geometry of the system orbit using all available relevant high-quality data. In Sect. 4 we determine the fundamental characteristics of the primary and secondary stars using constraints obtained from the spectroscopic and photometric data and show that these results are consistent with those determined from the orbital analysis. In Sect. 5 we model the geometry of the magnetic field of the Ap component. In Sect. 6 we discuss briefly the spectrum and rotation of the secondary. We then conclude in Sect. 7 with a summary of our results.

2. Observations

2.1. Magnetic field and polarisation measurements

2.1.1. UWO longitudinal field measurements

18 observations of the longitudinal magnetic field B_ℓ of HD 81009 were obtained using the University of Western Ontario (UWO) photoelectric polarimeter mounted on the 1.2 m telescope at the UWO Elginfield observatory. The polarimeter

was employed as a Balmer-line Zeeman analyser to measure the fractional circular polarisation in the wings of $H\beta$ at $\pm 5.0 \text{ \AA}$ from line centre. The instrument and observing technique are described in detail by Landstreet (1982). For HD 81009, a mean conversion factor (from measured circular polarisation to inferred longitudinal magnetic field) $\gamma = 16000 \text{ G per percent circular polarisation}$ was found from $H\beta$ line scans.

HD 81009 is an unresolved binary in the photoelectric polarimeter, with one magnetic component and one (presumably) non-magnetic component. Therefore the circular polarisation thus measured will be underestimated due to dilution by the flux of the non-magnetic star, resulting in an underestimate of the longitudinal field. The best available measurement of the magnitude difference between the two components is that from the Hipparcos catalogue (ESA 1997), which gives $\Delta H_p = 0.85 \pm 0.30$. The response peak of the H_p filter occurs near 5000 \AA ; therefore ΔH_p should provide a reasonably accurate estimate of the flux ratio at $H\beta$.

We have therefore corrected the photopolarimetric measurements for flux dilution by multiplying each measurement (as well as the associated uncertainty) by a factor $f = 1 + 10^{-\frac{\Delta H_p}{2.5}} = 1.5$ (e.g. Borra & Landstreet 1980). The inferred B_ℓ data, corrected for the flux dilution of the companion in this manner, are presented in Table 1.

2.1.2. ESO CASPEC longitudinal field measurements

13 measurements of the mean longitudinal magnetic field $\langle H_z \rangle$ of HD 81009 were obtained in the context of a larger study of magnetic fields in Ap stars (Mathys, Manfroid & Wenderoth 2000). The CASPEC spectrograph (the ESO Cassegrain Echelle Spectrograph) and Zeeman analyser were employed in order to simultaneously record spectra in both left and right circular polarisations. From each pair of orthogonally polarised spectra the longitudinal field was inferred from the relative shifts of spectral absorption lines. The observing, reduction and analysis procedures are described by Mathys & Hubrig (1997).

Because $\langle H_z \rangle$ is inferred from the relative *shifts* of spectral lines as viewed in the orthogonal polarisations, it is not affected by the continuum flux of the companion. However, measurement of $\langle H_z \rangle$ can be affected by the presence of the spectral *lines* of the secondary. Mathys (1990) searched for the lines of the secondary in spectra of HD 81009 without success. Examination of our spectroscopic data confirms this result. This is discussed in more detail later in this paper.

2.1.3. High-resolution intensity spectra and mean magnetic field modulus measurements

Thirty-nine high-resolution spectroscopic observations of HD 81009 were obtained by Mathys et al. (1997) in the context of a larger study of magnetic fields in Ap stars. Two additional observations were obtained by Mathys, Manfroid & Wenderoth (2000). From these spectra measurements of the mean magnetic field modulus $\langle H \rangle$ of HD 81009 were obtained, inferred from

fits to the magnetically-split components of the Fe II $\lambda 6149.2$ Zeeman doublet.

2.1.4. MuSiCoS spectropolarimetry

In addition a single series of spectropolarisation observations was obtained, in the context of a larger programme (Wade et al. 2000), using the MuSiCoS spectropolarimeter (Donati et al. 1999, mounted on the 2 metre Bernard Lyot Telescope at the Pic du Midi Observatory. The spectra, one in each of the V , Q and U Stokes parameters, cover the spectral range 4500–6600 Å with a resolution of around 35 000. Least-Squares Deconvolved (LSD) profiles obtained from these spectra exhibit unambiguous signatures in all Stokes parameters. For details concerning these data the reader should consult Wade et al. (2000).

2.2. Radial velocity measurements

Radial velocities (RVs) of HD 81009 have been measured from all of the spectroscopic data described above. In addition new RVs were obtained using the CORAVEL radial velocity scanner and CORALIE spectrograph. In total 72 new RV measurements of HD 81009 were obtained. Measurements from all sources are reported together in Table 2, available only in electronic form from the CDS by anonymous ftp 130.79.128.5. Here we describe briefly the details of the RV measurements.

12 RV measurements were obtained from CASPEC spectra and 36 RV measurements were obtained from the high-resolution intensity spectra. CASPEC RVs were inferred from a regression of measurements of the centres-of-gravity of absorption line profiles in the left and right circularly polarised spectra. RVs obtained from the high-resolution spectra were obtained by gaussian fitting of individual spectral features. The uncertainties in both cases are derived from the observed scatter of the measurements.

The MuSiCoS spectra were also used to obtain a single measurement of the RV of HD 81009. Using the Least-Squares Deconvolution procedure (Donati et al. 1997), a mean Stokes I profile (LSD profile; see Wade et al. 2000) was extracted using some 1600 lines in each échelle spectrum. The RV was obtained by measuring the centres-of-gravity of the mean profiles, and the average of the 3 measurements was adopted as the RV. The uncertainty is estimated based on the velocity stability of the spectrograph as determined using sharp-lined late-type stars.

2.2.1. RVs from the CORAVEL scanner and CORALIE spectrograph

The CORAVEL RV scanner (Baranne et al. 1979), installed on the Swiss 1 metre telescope at the Haute-Provence Observatory (OHP), was used between 1980 and 1999 to monitor the RV of HD 81009 as part of a larger programme aimed at monitoring magnetic Ap stars. The CORAVEL radial velocities are on the standard system defined by Mayor & Maurice (1985), which corresponds to the system defined by the faint IAU standard stars ($V > 4.3$). A total of 22 CORAVEL measurements of

HD 81009 were obtained, with a typical standard error under 1 km s^{-1} .

A single measurement of the RV of HD 81009 was obtained with the CORALIE spectrograph, recently installed on the Swiss 1.2 metre telescope at La Silla, Chile (Queloz et al. 1999). CORALIE operates in a fashion similar to CORAVEL, but achieves a higher spectral resolution (50 000) and hence somewhat higher RV precision.

All RV observations from 1980 to 1996 show only a very small variation (of about 2 km s^{-1}) which can be adequately explained as due to rotational modulation by surface structure on the Ap star (see Sect. 5). However, observations since 1996 show a steep and significant change in the RV, consistent with detection of the RV variation of HD 81009 due to its binary nature.

2.3. Astrometric data

2.3.1. Visual observations

The visual observations of the separation and position angle of the system began in 1905 (Aitken 1929) and were obtained regularly until 1970. For a good summary of the visual observations see van Dessel (1972).

During the phase when the component separation is the greatest $\rho \simeq 0.15$ arcsec, which is very difficult to observe visually. This problem is compounded by the fact that the two components have nearly identical visual magnitudes; thus the possibility of accidentally interchanging the components is quite severe.

When we attempt a preliminary model of the orbit using the visual observations we have difficulty obtaining a consistent solution. The recovered value of the eccentricity is small, between 0.04 and 0.22, and we believe this results from the difficulty of accurately identifying the two stars at phases when they are the closest. We thus conclude that the only reliable visual observations are those for which the component separation is large.

2.3.2. Speckle observations

From 1975 to 1994, 18 speckle observations of HD 81009 were obtained using the CHARA array by Hartkopf et al. (1998). These observations are of much higher quality than the visual observations, and provide the improved precision needed to follow the relative motion of this very close system. In addition a single unpublished CHARA observation was made available to us by W. Hartkopf.

2.3.3. Hipparcos observations

In addition to the large collection of data just described, one astrometric measurement of the separation and position angle of the HD 81009 system was obtained by the Hipparcos satellite (ESA 1997). This observation achieved a precision somewhat better than that typically achieved by Hartkopf et al. (1998). The

Table 3. Orbital parameters resulting from the combined modeling of the Hipparcos and CHARA astrometric measurements and the RV measurements, as well as parameters of orbits for HD 81009 published previously. Ω is the position of the ascending node (east of north), ω the longitude of the periastron, SA the semi major axis of the true orbit, $K1$ the radial velocity semi-amplitude for the primary and $K2$ the radial velocity semi-amplitude for the secondary, deduced from the speckle orbit and the Hipparcos (ESA 1997) parallax (7.20 ± 0.8 mas)

| Element | This study | Finsen (1968) | Starikova (1981) | van Dessel 1972) |
|--------------------------------|---------------------|---------------|------------------|------------------|
| P [years] | 29.30 \pm 0.27 | 22.3 | 53.422 | 58.93 |
| P [days] | 10673 \pm 99 | 8122 | 19459 | 21465 |
| T [HJD-2400000] | 50695 \pm 8 | 1948.6 | 1951.344 | 1944.0 |
| e | 0.718 \pm 0.006 | 0.95 | 0.044 | 0.219 |
| ω [°] | 134.24 \pm 0.77 | 90.0 | 127.9 | 262.44 |
| Ω [°] | 51.53 \pm 1.70 | 126.0 | 25.4 | 22.77 |
| SA [arcsec] | 0.1104 \pm 0.0027 | 0.1923 | 0.185 | 0.150 |
| i [°] | 138.6 \pm 1.8 | 66.4 | 69.4 | 56.09 |
| π [mas] | 7.2 \pm 0.8 | 16 | 8 | 5.6 |
| $K1$ [km s ⁻¹] | 6.80 \pm 0.09 | – | – | – |
| $K2$ [km s ⁻¹] | 10.75 \pm 2.77 | – | – | – |
| γ [km s ⁻¹] | 25.95 \pm 0.10 | – | – | – |
| M_A [M _⊙] | 2.6 \pm 1.5 | – | – | 2.77 |
| M_B [M _⊙] | 1.6 \pm 0.5 | – | – | 2.77 |
| $a_1 \sin i$ [AU] | 4.647 | – | – | – |
| $a_2 \sin i$ [AU] | 7.346 | – | – | – |

Hipparcos catalogue also provides the magnitude difference between the components ($\Delta H_p = 0.85 \pm 0.30$ mag) as determined from this single observation. The separation of the components of HD 81009 (0.1–0.15 arcsec) is near the limit of that which could be confidently measured by Hipparcos, hence the large error associated with the magnitude difference.

3. Orbit modeling

3.1. Previous solutions

A number of orbital solutions for HD 81009 have been published previously. These can be divided into two general categories based on the derived orbital period and eccentricity: longer-period, low-eccentricity orbits (van Dessel 1972; Starikova 1981) and shorter-period, high-eccentricity orbits (Finsen 1968). Examination of these orbits indicates that the principal ambiguity concerns the value of the orbital period, which is in any case quite long. Three periods have already been determined based on the visual astrometric observations: $P = 22.3$ years (Finsen 1968), $P = 53.422$ years (Starikova 1981) and $P = 58.93$ years (van Dessel 1972).

If we follow the lead of previous authors and consider only the visual astrometric observations, the orbital solutions of van Dessel (1972) and Starikova (1981) fit the observations satisfactorily. Finsen (1968) reversed the quadrant of a number of observations obtained at small separations (essentially switching the positions of the two stars) to obtain the period of 22.3 years. Since the publication of these papers the speckle astrometric observations were obtained, and these observations provide significantly more precise positions for the components. However, the speckle observations alone are still not sufficient to obtain a satisfactory solution, because these observations do

not cover the entire orbit, nor are they sufficient to determine the eccentricity.

The 72 new high-precision RV observations obtained in the context of this study provide crucial new constraint on the orbital motion. Although the new measurements are also insufficient, when considered alone, to determine unambiguously the orbital period (they as well do not cover a complete revolution of the system), the observed RV variation clearly implies an eccentricity greater than 0.5. If we use the four periods listed in Table 3 (the best-fit period based on our full solution described below, as well as those reported by earlier studies cited above) to fit spectroscopic orbits, we find that the inferred eccentricities span from 0.74 to 0.85. As it turns out, this new constraint on the orbit of HD 81009 is sufficient, when considered along with the speckle astrometric measurements, to remove all ambiguity concerning the orbital period and to allow us to determine a unique orbital solution for the system.

3.2. New orbital solution

The orbital solution is obtained by a method which combines the astrometric and radial velocity observations (Forveille et al. 1999). After a few initial attempts to reconcile all the astrometric observations, we decided to discard in their entirety the much lower quality visual astrometric observations.

For our final modelling of the orbit of HD 81009 we therefore employed only the Hipparcos and CHARA astrometric measurements, along with the 72 new RV measurements reported here. The least-squares fitting procedure converges smoothly to a solution with $P_{\text{orb}} = 29.30$ y, substantially different from that determined by any of the previous studies, but most similar to that of Finsen (1968). This method allows us to determine a consistent solution for all orbital parameters,

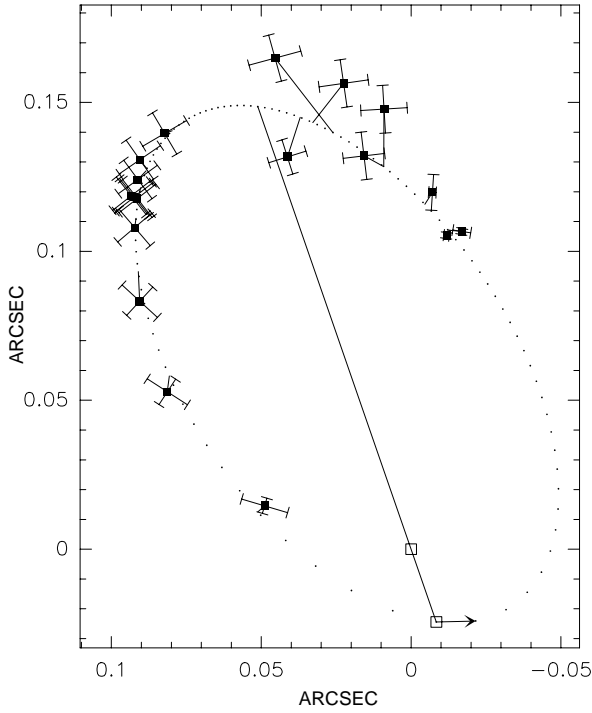


Fig. 1. Observed and calculated speckle astrometric positions of HD 81009. The dashed curve is the predicted orbital path of the secondary according to the new orbit described in Sect. 3.2 and in Table 3 (leftmost column). The solid line indicates the true semi-major axis of the orbit, while the arrow shows the motion of the secondary. Note the small predicted orbital separation at periastron, consistent with the accidental interchanging of the components that we propose contaminates the vi data

which are reported in Table 3. In Fig. 1 and Fig. 2 we compare the adopted orbit solution with the observations.

The component masses are also determined using this method, and are calculated using the orbital inclination and mass products. *A consistent orbit solution requires that the component for which RVs have been measured (the magnetic Ap star which generates the observed metallic absorption lines) be the primary component (i.e. the more massive star).* The relatively large errors on the inferred masses are due to the lack of radial velocity measurements of the secondary. Radial velocities for the secondary star would be very valuable for refining the speckle orbit and improving the mass determination. The RV variation of the secondary predicted assuming this model is also shown in Fig. 2. The primary RV residuals (shown in Fig. 6 in the context of a discussion of the variability of the Ap component) show no evidence for the presence of a tertiary component. The orbital solution also identifies the more massive Ap star as the *brighter* (in the H_p band) component of the system (already strongly suspected due to the domination of the line spectrum of HD 81009 by the lines of the Ap star).

The orbital analysis shows us that HD 81009 is a long-period ($P = 29.3$ y), highly eccentric ($e = 0.718$) binary system containing two components of similar mass ($\sim 2M_\odot$). This is consistent both with one component (the more massive star) being a

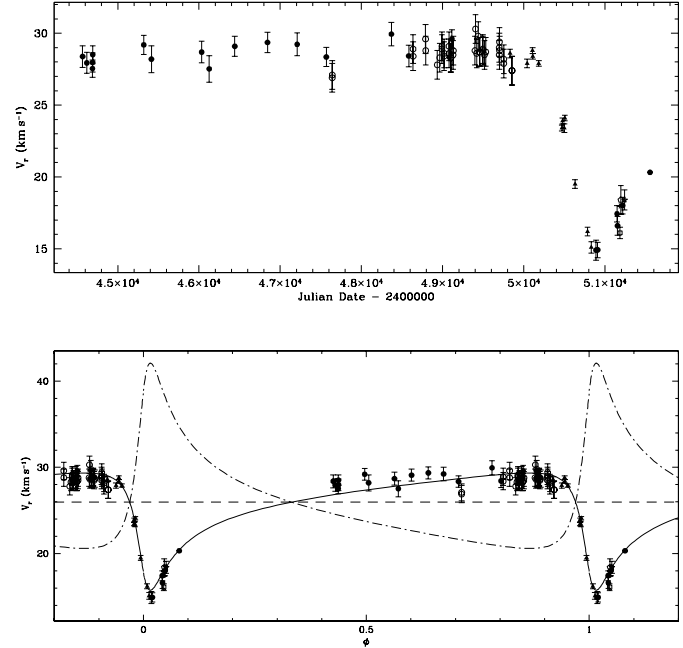


Fig. 2. Observed RVs of HD 81009. *Upper frame* – RV versus Julian Date *Lower frame* – RVs phased according to the new orbital ephemeris described in Sect. 3.2 and in Table 3 (leftmost column). The solid curve is the RV variation of the primary calculated from the adopted orbit model, while the dashed curve is that predicted for the secondary

magnetic Ap star, and with the small component magnitude difference as observed by Hipparcos. Because all known magnetic Ap stars are main sequence stars, it probably implies that both components are main-sequence A stars. The minimum orbital separation of the system is $d_{\min} = (a_p + a_s)(1 - e) = 5.1 \text{ AU} \simeq 760 R_\odot$, and if both stars are main sequence A stars this would imply that both components have evolved independently (i.e. as single stars, as $R_*/d_{\min} \ll 1\%$).

4. Component characteristics

The component masses determined via the orbital analysis are somewhat approximate. In this Section we will employ the spectral energy distributions and high-resolution spectra to provide independent constraints on their physical parameters.

4.1. A search for the spectral lines of the secondary

As discussed earlier in this paper, Mathys (1990) searched unsuccessfully for the spectral lines of the secondary in a sample of high resolution spectra. In this Section we also attempt such a search, using both multi-line and single-line strategies.

We begin with cross correlation-type analyses of the CORAVEL, MuSiCoS and CORALIE spectra. Neither the CORAVEL nor CORALIE autocorrelation profiles, nor the MuSiCoS LSD mean Stokes I profiles show any indication of the secondary. The larger CORAVEL radial velocity window covers a range of 120 km s^{-1} , the CORALIE radial velocity window cover a range of 200 km s^{-1} , and the MuSiCoS LSD profiles

were computed using both 240 km s^{-1} and 600 km s^{-1} deconvolution windows. Both CORAVEL and MuSiCoS have been used previously to detect weak lines due to binary companions (e.g. Wade et al. 1996; Wade 1998).

A careful examination of the lines in the CASPEC and the high-resolution spectra for the metal lines of the secondary was unsuccessful. Furthermore, no features in the CORALIE or MuSiCoS $H\alpha$ or $H\beta$ profiles could be conclusively identified with the secondary, and the core wavelengths of those lines are consistent within the uncertainties with the RV as measured using metallic lines (i.e. the RV of the Ap star). This is not surprising – the separation of the components in radial velocity at this phase is only about 20 km s^{-1} , and would be very difficult to detect in such a broad line. Furthermore, our difficulty detecting the metallic lines of the secondary is also not unexpected, given the remarkable richness of the spectrum of HD 81009 (illustrated in Fig. 3).

Thus we find no evidence of the spectral lines of the secondary in our spectra of HD 81009. We will revisit this result later in the paper.

4.2. Relative and absolute luminosities of the components

Gomez et al. (1998) included HD 81009 in their study of the H-R diagram position of Ap stars. To account for the flux contribution of the secondary component, Gomez et al. corrected the apparent magnitude of HD 81009 by -0.7 mag (Gomez 2000, priv. comm.). Taking the absolute magnitude reported by Gomez et al. (1998; determined using the L-M method) and removing this correction, we obtain for the absolute magnitude of the HD 81009 system $M_V = 0.52 \pm 0.25$ mag.

The component masses, the combined spectral type and the magnitude difference all suggest that both components are main sequence A stars. The bolometric correction relation for such stars is flat and essentially gives $BC = 0$ (e.g. Code et al. 1976). Assuming $BC = 0$ for both components, $M_{\text{bol}} = M_V$, and the luminosity of the system is then:

$$L_{\text{sys}} = 10^{-\left(\frac{M_{\text{bol}} - M_{\text{bol}}^{\odot}}{2.5}\right)} = 47.4_{-9.7}^{+12.3} L_{\odot}, \quad (1)$$

for $M_V^{\odot} = +4.71$ (Gray 1992). According to the observed magnitude difference the luminosity of the primary component is:

$$L_p = \left(\frac{L_p}{L_{\text{sys}}}\right) \cdot L_{\text{sys}} \quad (2)$$

$$= \frac{L_{\text{sys}}}{\frac{\Delta M_{\text{bol}}}{1 + 10^{-\frac{\Delta M_{\text{bol}}}{2.5}}}}, \quad (3)$$

giving $L_p = 32.5_{-9.0}^{+11.8} L_{\odot}$. The luminosity of the secondary is then $L_s = L_{\text{sys}} - L_p = 14.9_{-5.2}^{+7.5} L_{\odot}$. These luminosities are indeed consistent with A-type main sequence stars with masses of around 2.2 and $1.9 M_{\odot}$.

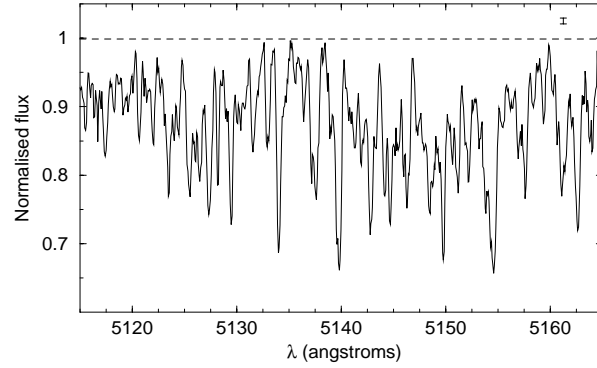


Fig. 3. A typical 50 \AA region of the optical spectrum of HD 81009, illustrating the challenge of detecting the metallic absorption lines of the secondary. The noise level is represented by the error bar at upper right

4.3. Effective temperatures of the components

In this Section we will attempt to determine the effective temperatures of the components by modelling the optical spectral energy distributions (SEDs) of HD 81009 obtained by Adelman (1981), using binary star flux models produced from Atlas9 fluxes (Kurucz 1993).

The observed SEDs show a scatter of $0.03\text{--}0.05$ mag which may in part be due to rotational modulation. The model fluxes are compared with all SEDs (i.e. all rotational phases) simultaneously; the scatter provides some estimate of the uncertainty associated with fitting the models.

For completeness, we begin by noting that the SED of HD 81009 is reasonably consistent with a single star model with effective temperature $T_{\text{eff}} = 8250 \text{ K}$ and surface gravity $\log g = 4.0$, assuming a metallicity enhanced 10 times over solar and 2 km s^{-1} microturbulence; i.e. as in the optical spectra, there is no strong evidence for binarity in the SED. While clearly inconsistent with the RV, photometric and astrometric measurements, this single star model provides a good point from which to begin our exploration of the agreement of the SED with binary star models.

For our initial binary model we select a primary star with parameters the same as those as described in the single star model above, and a somewhat cooler secondary with $T_s = 7000 \text{ K}$, $\log g = 4.0$, solar metallicity and 2 km s^{-1} microturbulence. We furthermore adopt the component luminosities derived in Sect. 4.2. Recall that the information about the secondary contained in the SED appears to be quite limited; it is only by requiring simultaneous consistency between the observed and predicted luminosities and the SED that we can obtain useful constraint on the temperature of the secondary.

These initial luminosities and effective temperatures correspond (according to the model evolutionary calculations for solar metallicity by Schaller et al. 1992) to component masses of 1.8 and $2.2 M_{\odot}$ and a ratio of radii $R_p/R_s \simeq 1.1$. Using the ratio of radii to translate the Atlas9 fluxes (in units of $\text{erg cm}^{-2} \text{ s}^{-1} \text{ Hz}^{-1}$) into intensities (units of $\text{erg s}^{-1} \text{ Hz}^{-1}$), we calculate the theoretical SED expected for this model.

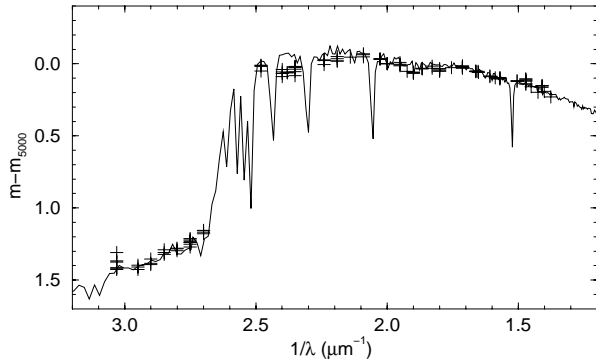


Fig. 4. Spectral energy distribution of HD 81009 obtained by Adelman (1981). The solid curve represents the adopted ($T_{\text{eff}} = 8500$ K, $\log g = 4.0$, $Z = 10 Z_{\odot}$) + ($T_{\text{eff}} = 7750$ K, $\log g = 4.0$, $Z = Z_{\odot}$) binary flux model

This initial model matches well the observed SED up to about 500 nm, but the calculated slope of the Paschen continuum is too gentle. A somewhat hotter model with primary $T_p = 8500$ K and secondary $T_s = 7250$ K provides a much better fit, with only a small discrepancy in the Paschen continuum slope. The agreement is satisfactory for a ($T_p = 8500$ K, $T_s = 7750$ K) model, with both stars having $\log g = 4.0 \pm 0.2$. The observed SED is compared in Fig. 4 with that calculated using this binary model. These atmospheric parameters, when considered along with the component luminosities determined in Sect. 4.2, correspond to respective primary and secondary masses of 2.20 and 1.84 M_{\odot} (according to the model evolutionary calculations of Schaller et al. 1992), and respective radii of 2.6 and 2.2 R_{\odot} . These masses and radii result in “evolutionary” logarithmic surface gravities of 4.0 for both stars, in perfect agreement with the “spectroscopic” surface gravities inferred from the SED. The luminosity ratio resulting from the adopted binary model is $L_p/L_s = 2.0$, equivalent to a magnitude difference $\Delta V = 0.75$ mag, well within the ± 0.3 mag error bar associated with the observed magnitude difference.

This procedure shows that the SED and component magnitude difference of HD 81009 are consistent with both components being main sequence A stars, a combination that we have argued is the most probable system configuration given the independent requirements that the magnetic star is probably an A-type main sequence star, that the magnetic star is the more massive and brighter component, and that the component masses are $M_{pri} = 2.6 \pm 1.5 M_{\odot}$ and $M_{sec} = 1.6 \pm 0.5 M_{\odot}$ (deduced from the orbital analysis in Sect. 3.2). We find no other combination of components which satisfies these various requirements; the error bars associated with the inferred luminosities and effective temperatures accurately illustrate the region of the H-R diagram for which the observed magnitude difference and SED are simultaneously satisfied by the model.

In Fig. 5 we compare the composite $H\alpha$ line profile predicted by our adopted binary model with the observed profile from our single Coralie spectrum. As discussed earlier, no clear asymmetry or shift is evident in the observed profile. The composite model profile was calculated from the sum of Atlas9

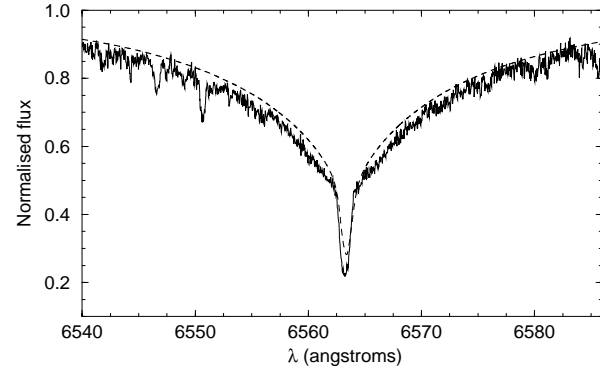


Fig. 5. Comparison of the observed $H\alpha$ profile of HD 81009 with the composite profile computed assuming the adopted component characteristics and the orbital radial velocities at this orbital phase (about $\phi = 0.02$). The agreement is satisfactory, although the observed core is somewhat deeper than that predicted by the model

Table 4. Derived basic physical properties of the components of HD 81009

| | Primary | Secondary |
|-----------------------------------|-----------------------|----------------------|
| T_{eff} (K) | 8500 ± 250 | 7750 ± 400 |
| L/L_{\odot} | $32.5^{+11.8}_{-9.0}$ | $14.9^{+7.5}_{-5.2}$ |
| R/R_{\odot} | 2.6 ± 0.5 | 2.2 ± 0.5 |
| $\mathcal{M}/\mathcal{M}_{\odot}$ | 2.20 ± 0.2 | 1.84 ± 0.2 |
| $\log g$ | 4.0 ± 0.2 | 4.0 ± 0.2 |
| $\log \text{Age}(\text{y})$ | 8.66–8.82 | 8.2–9.0 |

Balmer α profiles (Kurucz 1993) appropriate to our model binary components, weighted according to the derived flux ratio and shifted according to the component radial velocities (determined from the orbital model). The agreement in the wings is good, although the core depth is somewhat underreproduced by the model. We find that we can improve the agreement in the line core by decreasing the separation in wavelength of the two components’ lines, i.e. by reducing the radial velocity separation between the two stars. One interpretation of this is that the mass ratio $\mathcal{M}_p/\mathcal{M}_s$ is somewhat smaller (i.e. closer to 1.0) than is predicted by the orbital model. This is consistent with the masses derived spectroscopically, which give a mass ratio of 1.2, versus 1.6 from the orbital masses.

Finally, we find that the derived H-R diagram positions of the components (shown in Fig. 6) are consistent with a co-eval system, both components’ 1σ error boxes intersecting isochrones for $\log \text{Age}(\text{y}) = 8.66\text{--}8.82$ (these values are defined by the somewhat smaller error box of the primary). This reasonable result further supports our conclusion. The basic physical properties of the components of the HD 81009 system are summarised in Table 4.

5. Rotation and magnetic field of the primary

Based on the orbital and spectral analysis presented above we have concluded that the primary is responsible for the observed

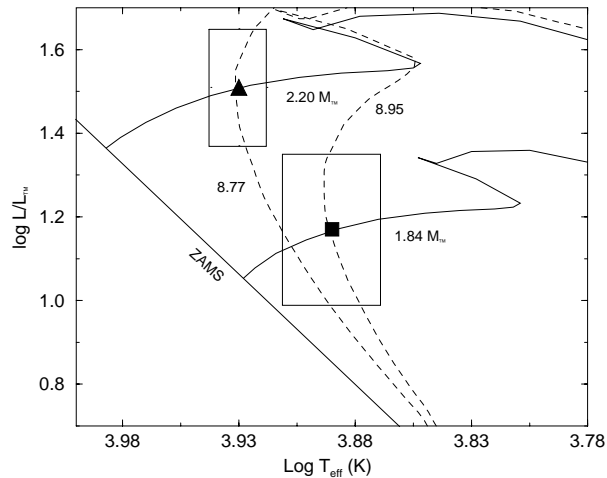


Fig. 6. H-R diagram ($\log T_{\text{eff}}$ vs. $\log L/L_{\odot}$) showing the positions of the primary and secondary components of HD 81009. Also shown are evolutionary tracks for 1.84 and 2.20 M_{\odot} , and isochrones corresponding to $\log(\text{Age}) = 8.65, 8.77$, and 8.95

spectral lines of HD 81009, and is therefore the identified variable magnetic chemically peculiar star.

5.1. Rotational period

Adelman (1997) performed a careful analysis of the rotational period of HD 81009 using 253 Strömgren photometric measurements, archival Strömgren photometry published by Wolff (1975) and Hensberge et al. (1981), as well as Geneva photometry obtained by Waelkens (1985). Adelman reports that these data are consistent with a unique period of $33^{\text{d}}984 \pm 0^{\text{d}}002$.

An examination of the periodogram of the field modulus $\langle H \rangle$ measurements shows a single strong peak, and uniquely determines the period to be $33^{\text{d}}972 \pm 0^{\text{d}}055$. This period is consistent with that determined from the photometric measurements.

As the longitudinal field measurements have neither sufficient time span nor sufficient S/N to uniquely determine the period, we adopt the more precise photometric ephemeris (Adelman 1997):

$$\text{JD}(v \text{ max.}) = 2444483.42 \pm 0.04 + 33^{\text{d}}984 \cdot E, \quad (4)$$

where phase 0.0 refers to the epoch of Strömgren v maximum light.

When the magnetic data are phased according to the rotational ephemeris, all three data sets describe smooth, approximately sinusoidal variations and result in reduced χ^2 s near 1.0 when fit with sine curves. A possible anharmonicity may exist in the phased B_{ℓ} measurements. However, first and second-order sine fits to the B_{ℓ} data both yield reduced χ^2 s of 0.8, indicating that any anharmonicity is insignificant at the level of precision of the data.

There exists a clear difference in the amplitude of the two longitudinal field curves. Such differences between B_{ℓ} and $\langle H_z \rangle$ measurements are not uncommon (e.g. Wade et al. 1997), although they may be compounded in this case by uncertainties

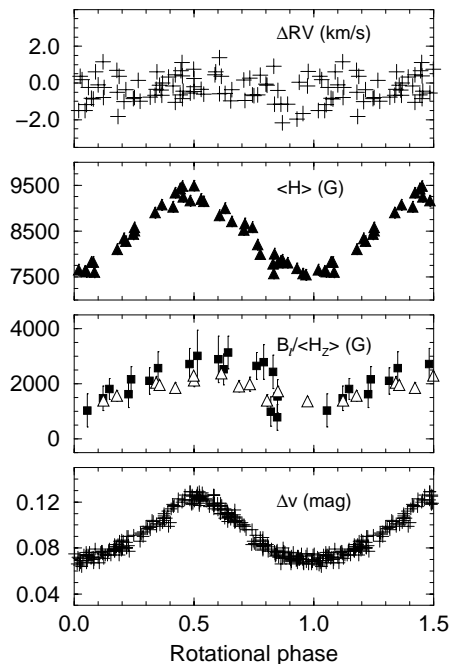


Fig. 7. Observed RV residuals (after subtraction of the primary orbital RV variation discussed in Sect. 3.2), mean field modulus measurements (second from top), longitudinal field measurements (third from top, squares= B_{ℓ} , triangles= $\langle H_z \rangle$), and v -band photometric variation (bottom; Adelman 1997) of HD 81009, phased according to the ephemeris described in the text

associated with the component magnitude difference. However, we point out that no uniform scaling of the B_{ℓ} variation results in congruence with the $\langle H_z \rangle$ variation; there are clearly systematic differences between the two curves which appear to be unrelated to any uncertainties associated with flux dilution.

The RV residuals (first discussed in Sect. 3.2) have also been phased according to Adelman's ephemeris. No coherent variation is detected in these data, and any modulation is limited to about $\pm 2 \text{ km s}^{-1}$.

The phased longitudinal field and mean field modulus measurements, along with the v -band photometry (Adelman 1997) and the RV residuals, are all shown together in Fig. 7.

5.2. Surface magnetic field geometry

Using a computer programme which assumes a decentred dipole magnetic field, we have synthesized longitudinal field and mean field modulus variations for a range of magnetic field models. The four free parameters in the models are the inclination of the stellar rotational axis to the observer's line of sight i , the inclination of the magnetic dipole axis to the rotational axis β , the polar strength of the magnetic dipole (when centred) B_{d} , and the decentring a of the magnetic dipole as a fraction of the stellar radius, in the direction of the magnetic axis. These four parameters are determined formally by our four independent observational constraints on the magnetic field: the (two) extrema of the average longitudinal field and the (two) extrema of the mean field modulus curve. Because of the large differences between the

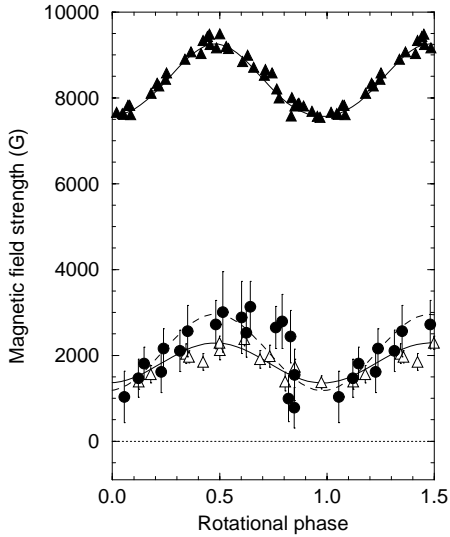


Fig. 8. Phased mean field modulus and longitudinal field measurements. The curves are the variations produced by the magnetic models described in the text: solid curve= $\langle H_z \rangle$, dashed curve= B_ℓ . Note the difference in amplitude between the B_ℓ (circles) and $\langle H_z \rangle$ (triangles) variations

B_ℓ and $\langle H_z \rangle$ curves we will model them separately. Searching parameter space for those models consistent with the observations, we find the best agreement between the observed and computed variations for the following parameters: $\langle H \rangle + B_\ell$: $(i/\beta, \beta/i) = (19^\circ, 130^\circ)$, $B_d = -10.9$ kG, and $a = -0.07$; $\langle H \rangle + \langle H_z \rangle$: $(i/\beta, \beta/i) = (12^\circ, 133^\circ)$, $B_d = -8.5$ kG, and $a = -0.23$. The phased magnetic field data are compared with the results of the model computations in Fig. 8. Clearly the important systematic differences between the B_ℓ and $\langle H_z \rangle$ data translate into large differences in the recovered field configurations.

The ambiguity which exists between the two angular parameters i and β is a fundamental result of such an axisymmetric magnetic field, and for stars with small $v \sin i$ it can usually only be resolved using linear polarisation observations. However, Mathys, Manfroid & Wenderoth (2000) report a significant crossover $v \sin i \langle x H_z \rangle$ for this star. Given that the HD 81009 is truly a slow rotator ($P \sim 34$ days; as opposed to being a rapid rotator seen pole-on), this suggests that the $v \sin i$ of this star is not insignificant and therefore that the inclination i is most probably the larger angle. This is supported by the low expectation value of stars with small i ($P(i < 20^\circ) \simeq 6\%$). We therefore conclude that, for both data sets, i is most probably the larger angle and β the smaller. We can test this conclusion by checking whether the projected rotational velocity resulting from the adopted i , R and P_{rot} is consistent with the observed $v \sin i$ of HD 81009 ($\lesssim 5 \text{ km s}^{-1}$). $v \sin i$ is determined using the expression:

$$\frac{R}{R_\odot} = \frac{P \cdot v \sin i}{50.6 \cdot \sin i}, \quad (5)$$

and we find $v \sin i = 2.8 \text{ km s}^{-1}$ for both data sets, which is consistent with the observed value, as well as with any modulation present in the RV residuals.

6. Rotation and spectrum of the secondary

As was discussed in Sect. 4.1, no unambiguous spectroscopic signature of the secondary is detected in our data. However, the astrometric, photometric and RV observations unambiguously require the presence of the companion. Based on this requirement and the additional constraint provided by our spectroscopic data we have determined a unique solution for the physical properties of the secondary which are summarised in Table 4.

Recall that the MuSiCoS spectra of HD 81009 have been analysed using the Least Squares Deconvolution (LSD) multiline procedure which produces a “mean” profile for each of the Stokes parameters (including Stokes I). No signature of the secondary was detected in the LSD mean profiles.

If we assume that the mean line of the secondary has the same intrinsic strength as that of the primary, and is rendered weaker only due to the primary’s greater relative flux, we can very approximately estimate the projected rotational velocity of the secondary. For a secondary $v \sin i = 2.8 \text{ km s}^{-1}$ (identical to that of the primary) the secondary’s mean line should be detectable (due to line doubling) on the date the MuSiCoS observation was obtained. Clearly this is not the case. However, for secondary $v \sin i \gtrsim 15$ or 20 km s^{-1} detection of its mean line would be ambiguous, as it would be only about 15% as strong as the primary’s line, and would lie well within the primary line’s (magnetically-broadened) wing. It therefore appears that the simplest explanation for the lack of spectroscopic evidence of the secondary is that the secondary rotates somewhat more rapidly than the primary, with $v \sin i$ at least $15\text{--}20 \text{ km s}^{-1}$.

7. Summary

In this paper we have analysed the orbit and component characteristics of the binary system HD 81009, as well as the magnetic field of the Ap star primary component.

We began by determining the orbital geometry of HD 81009 by simultaneously fitting new and archival radial velocity and astrometric measurements. The resultant solution has a period of 29.3 years, is highly eccentric ($e = 0.718$) and is similar in this respect to a solution determined previously by Finsen (1968). Our data are not consistent with previously published solutions with periods of 50–60 years, such as those of van Dessel (1972) and Starikova (1981). The orbit model also provides us with some constraint on the component masses, which are found to be $1.6 \pm 0.5 M_\odot$ and $2.6 \pm 1.5 M_\odot$.

Our next step was to constrain the luminosities, effective temperatures and surface gravities of the components by simultaneously satisfying the observed magnitude difference ($\Delta H_p = 0.85$; ESA 1997) and the spectral energy distribution obtained by Adelman (1987). From this procedure we obtain strong constraints on the physical properties of the components,

determining that they are both main sequence A stars with effective temperatures of 7750 and 8500 K.

We then proceeded to study in detail the rotation and magnetic field of the Ap star primary. Adopting a previously determined photometric period (consistent with all available data) as the rotational period, we report the rotational variation of the mean magnetic field modulus and the mean longitudinal magnetic field. These data have been modelled assuming a decentred dipole magnetic field. The magnetic obliquity determined from this modeling is $\beta < 20^\circ$, implying that the magnetic field axis of the primary is approximately aligned with its rotational axis. This is consistent with the results of Landstreet & Mathys (2000), who find that this is a general property of slowly-rotating magnetic Ap stars.

Acknowledgements. GAW acknowledges support from the Natural Sciences and Engineering Research Council of Canada (NSERC) in the form of a Postdoctoral Fellowship and research support from the NSERC Operating Grants of J.B. Lester and C.T. Bolton. JDL acknowledges support from NSERC in the form of an Operating Grant. The work of YD has been supported by continuous grants from the Swiss National Foundation for Scientific Research (FNRS). Thanks to W.I. Hartkopf for sharing details of unpublished CHARA observations of HD 81009. This work has made use of the SIMBAD database and Hipparcos databases via the Canadian Astronomy Data Centre (CADC).

References

- Abt H.A., 1981, *ApJS* 45, 437
 Abt H.A., Conti P.S., Deutsch A.J., Wellerstein G., 1968, *ApJ* 153, 177
 Abt H.A. & Snowden M.S., 1973, *ApJS* 25, 137
 Adelman S.J., 1981, *A&AS* 43, 183
 Adelman S.J., 1997, *PASP* 109, 9
 Aitken R. G. 1929, *Lick Obs. Bull.* 14, 73
 Baranne A., Mayor M., Poncet J.-L. 1979, *Vistas in Astron.* 23, 279
 Bolton, C. T., Harmanec, P., Lyons, R. W., Odell, A. P. & Pyper, D. M. 1998, *A&A* 337, 183
 Bonsack W.K., 1976, *ApJ* 209, 160
 Borra E.F. & Landstreet J.D., 1980, *ApJS* 42, 421
 Code A.D., Bless R.C., Davis J., Brown R.H., 1976, *ApJ* 203, 417
 Cowley A., Cowley C., Jaschek M., Jaschek C., 1969, *AJ* 74, 375
 Donati J.-F., Semel M., Carter B.D., Rees D.E., Cameron A.C., 1997, *MNRAS* 291, 658
 Donati J.-F., Catala C., Wade G.A., Gallou G., Delaigue G., Rabou P., 1999, *A&AS* 134, 149
 ESA. 1997, *The Hipparcos and Tycho Catalogues (ESA SP-1200)* (Noordwijk: ESA)
 Finsen W.S., 1968, *Repub. Obs. Johannesb. Circ.*, 7, 170
 Forveille T., Beuzit J.-L., Delfosse X., Segransan D., Beck F., Mayor M., Perrier C., Tokovinin, A., Udry S., 1999, *A&A* 351, 619
 Gomez A.E., Luri X., Grenier S., Figueras F., North P., Royer F., Torra J., Messier M.O., 1998, *A&A* 336, 953
 Gray D.F., 1992, *The Observation and Analysis of Stellar Photospheres*, Cambridge University Press
 Hartkopf W. I., McAlister H.A., & Mason B.D. 1998, *Third Catalog of Interferometric Measurement of Binary Stars*, CHARA Contribution No. 4, Georgia University.
 Hensberge H. Deridder G., Doom C., Maitzen H.M., et al., 1981, *A&AS* 46, 151
 Kurucz R.L., 1993, CD-ROM #13
 Landstreet, J.D., 1982, *ApJ* 258, 639
 Landstreet J.D. & Mathys G., 2000, *A&A*, in press
 Mathys G., 1990, *A&A* 232, 151
 Mathys G. & Hubrig S., 1997, *A&AS* 124, 475
 Mathys G., Hubrig S., Landstreet J.D., Lanz T., Manfroid J., 1997, *A&AS* 123, 353
 Mathys G., Manfroid J., Wenderoth E., 2000, in preparation
 Mayor M., Maurice E. 1985, in *IAU Coll. 88*, Eds A.G.D. Philip & D.W. Latham L. Davis Press (Schenectady, N.Y.), p. 35
 North P., 1994, in *The 25th workshop and meeting of European working group on CP stars*, eds. I. Jankovics and I.J. Vincze, Gothard Astrophysical Observatory of Eötvös University, Szombathely, Hungary, p. 3
 Queloz D., 2000, in preparation
 Schaller G., Schaerer D., Meynet G., Maeder A., 1992, *A&AS* 96, 269
 Starikova G.A., 1981, *Sov. Astron. Letters* 7, 130
 van Dessel E.L., 1972, *A&A* 21, 155
 Wade G.A., Elkin V.G., Landstreet J.D., Romanyuk I.I., 1997, *MNRAS* 292, 748
 Wade G.A., 1998, Ph.D. Thesis, The University of Western Ontario
 Wade G.A., Mathys G., North P., Hubrig S., 1996, *A&A* 314, 491
 Wade G.A., Donati J.-F., Landstreet J.D., Shorlin S.L.S., 2000, *MNRAS* 313, 823
 Waelkens C., 1985, *A&AS* 61, 127
 Wolff S.C., 1975, *ApJ* 202, 127